HEATING CHARACTERISTICS OF A PLASMA ARC

S. M. De Almeida and B. K. Hinds
Department of Mechanical and Industrial Engineering
The Queen's University of Belfast

ABSTRACT

A method is presented here which allows the determination of the heat flux distribution under a plasma arc column, to a rotating anode. This is carried out using a thermocouple embedded in the anode as a sensing probe which makes successive passes under the arc at known off-sets from the arc centre. The information extracted from this, taken together with the efficiency of heat transfer found calorimetrically is used to arrive at the flux distribution.

1. INTRODUCTION

The plasma arc is frequently used in many industrial applications such as welding, heating or hot machining. The effect required in these processes is a transfer of energy from the arc to a localised area on the material under the arc. In order to apply the right torch conditions to a particular process, it is required to know the heat energy concentration and its distribution. In previous investigations of the arc (Plasma and TIG), the methods adopted have been the use of split plate anodes and thermal probes in anodes (1, 2). In these cases the arc were maintained stationary relative to a water cooled anode. The work by Rykalin (2) indicated that the heat flux distribution is of the Gaussian form, which is the form assumed by other investigators, Pavelic et al (3) and Friedman et al (4). However, Nestor (1) has stated that these distributions are sharper than Gaussian.

The main purpose of the investigation reported here is to develop a simple experimental method of determining the heat flux distribution under an arc.

2. EXPERIMENTAL METHOD

The basic principle of the method is that a strip of the area covered by the plasma arc is made to traverse over an exposed thermocouple during a short interval of time. This interval is made short enough so as to cause no surface melting and that the overall temperature rise in the thermocouple to remain small. The average temperature rise of the thermocouple is proportional to the heat received by the bead during the traverse time. If the plasma arc spot is scanned in the above manner consecutively, the profile of the temperature rise reflects the heat flux distribution considered as a line source. The actual radial flux distribution can then be computed from the knowledge of the efficiency of heat transfer of the arc and by using the Abel transformation technique.

To achieve this, a thermocouple (0.5 mm bead dia) was mounted on a large disc held in a lathe with the thermocouple bead flush with the face of the disc and in contact with the disc so that bead itself was part of the anode.

The cross feed mechanism of the lathe was used to move the plasma arc relative to the thermocouple while the disc was rotating. The full experimental arrangement is shown in figure 1a. The configuration used for the measurement of efficiency is shown in figure 1b. The heat transfer efficiency (the arc efficiency - defined as the ratio of the heat energy received by the workpiece to the gross power input) was calculated using the central portion of the workpiece in calorimetric test.

3. RESULTS AND DISCUSSION

This method of determining the heat flux distribution makes the following assumptions :

(i) the mass of the thermocouple bead remains unchanged throughout the experiment, i.e. no evaporation or melting takes place under the plasma arc.

(ii) the thermal capacity of the bead remains constant.

(iii) the average temperature rise in the bead is small (i.e. achieved by keeping the traverse time short).

(iv) the thermal inertia of the thermocouple is not large.

(v) losses from the thermocouple bead during the rise time are not significant.

From the trace of temperature rise for the full scan of the arc spot (fig 2), it is seen that the maximum temperature rise (XY in fig 2) is small compared with the melting point of the thermocouple material. The path indicated by line A is the temperature rise of the ceramic cement surrounding the bead. The temperature of the bead continues to rise for a short duration after passing through the plasma before falling gradually to the bulk temperature of the ceramic insulator. All of the assumptions made are seen to be justified from the examination of the temperature rise in the thermocouple and the repeatability of the experiment. As the thermocouple bead itself forms a part of the anode, the heat energy transfer from electron effects at the anode are also taken into account. Further, as only a relative distribution is required, errors due to heat losses and those caused by having a material different from the workpiece as the thermal probe will not be significant as they are of the same order during each rise time.

The plot of temperature rise against the distance across the arc gives the relative net strength of the arc for a given gross power input. The area under this curve is proportional to the net power of the arc calculated using the efficiency of heat transfer found by the calorimetric experiments (5). Figure 3 shows the heat flux distribution (regarded as a line source) across the arc for a particular set of parameters. The skewness of the distribution in the direction away from the direction of feed is caused by the deflection of the plasma column towards the heated metal due to thermionic effects. The first half of the curve can be taken to be representative of the actual heat flux profile and the error would be in the order of 7%. With this assumption, a curve fitting technique (interactive curve-fit programme on Imlac/ICL 1906S computers using the method of least squares) was employed to find an equation for the curve. This distribution so obtained represents a line source, i.e. an individual point on the curve represents the integration of the heat absorbed along a chord of the actual 3-dimensional flux distribution. The actual radial distribution (assumed to be radially symmetrical) was computed applying the Abel's transformation algorithm developed by Bockasten (6). In general the radial heat flux distribution of the plasma arc was found to be describable by an equation of the Super-Gaussian type -

$$q_r = \text{Exp}\ (A - Br^2 + Cr^4 - Dr^6)$$

where r is the radial distance and A, B, C and D are constants.

Figure 4 shows the variation of the net heat density distribution with the increase of the gross power into the arc for a given set of parameters. Table 1 gives the values of coefficients of the equation (1) in respect of the curves shown in figure 4.

In conclusion, it can be said that the method used enables one to find the net heat flux distribution of an arc very conveniently and accurately. Further, the effects of having large insulated probes or the edge effects found in other methods are eliminated.

REFERENCES

(1) O.H. Nestor, Physics of Welding arc - a Symposium, Inst. of Weld. London, October 1962.

(2) N.N. Rykalin, I.D. Kulagan, A.V. Nivkolaev, Avt. Svarka, USSR, 1963, No 6, pp 3-13.

(3) V. Pavelic, R. Tanbakuchi, O.U. Uyehara, Weld. J. Res. Suppl. Vol 48, No 7, 1969, pp 295S-305S.

(4) E. Friedman, S. S. Glickstein, Weld. J. Res. Suppl. Vol 55, 1976, pp 408S-420S.

(5) S.M. De Almeida, 'Plasma assisted hot machining', Ph.D. Thesis, The Queen's University of Belfast, 1980.

(6) K. Bockasten, J. of the Optical Society of America, 1961, Vol 51, No 9, pp 943-947.

TABLE I

Constants of equation (1) $q_r = \text{Exp}(A - Br^2 + Cr^4 - Dr^6)$ watts/mm², where r is the radial distance in mm. Curve fit produces RMS error less than 0.7% of the maximum ordinate.

Gross Power in kW	Efficiency	A	B	C	D
2.0	0.34	3.7397	0.2179	2.5136×10^{-4}	7.829×10^{-5}
3.11	0.45	4.388	0.2724	1.584×10^{-2}	5.361×10^{-4}
4.4	0.50	4.932	0.2974	1.0196×10^{-2}	1.3956×10^{-4}
5.75	0.54	5.261	0.3084	1.1195×10^{-2}	1.743×10^{-4}
7.2	0.55	5.40	0.2747	8.469×10^{-3}	9.396×10^{-5}
8.40	0.57	5.535	0.1996	3.310×10^{-3}	1.992×10^{-5}

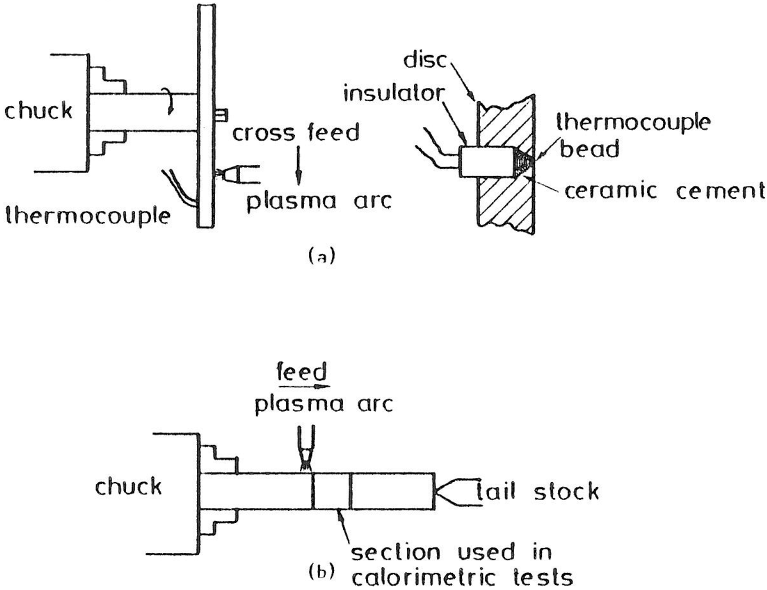

Figure 1 Experimental Configuration

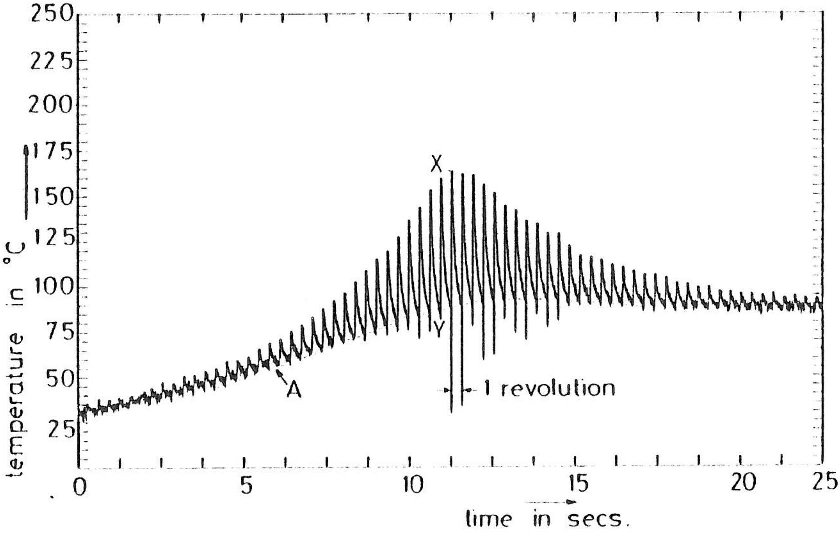

Figure 2 Thermocouple response during test

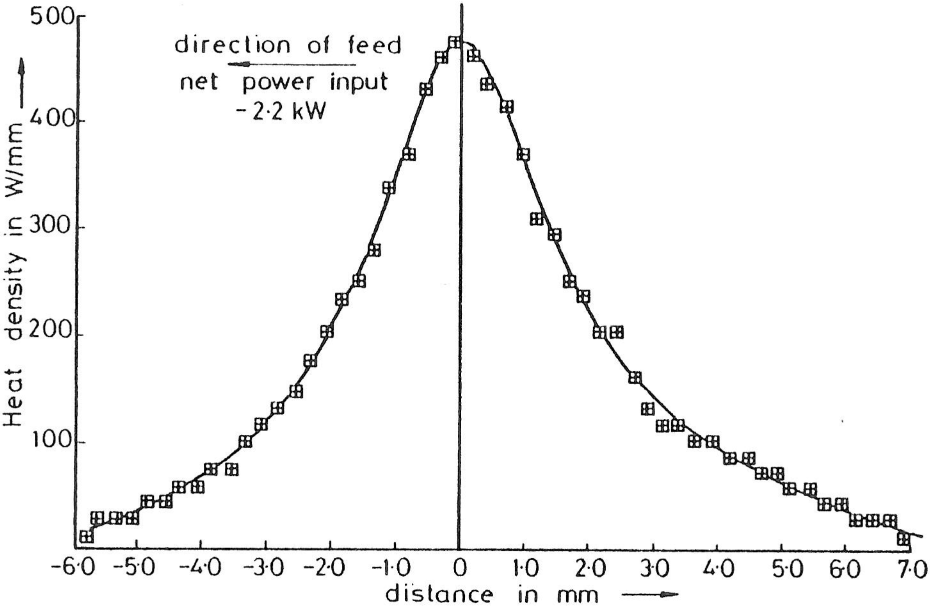

Figure 3 Derived heat density profile (as a line source)

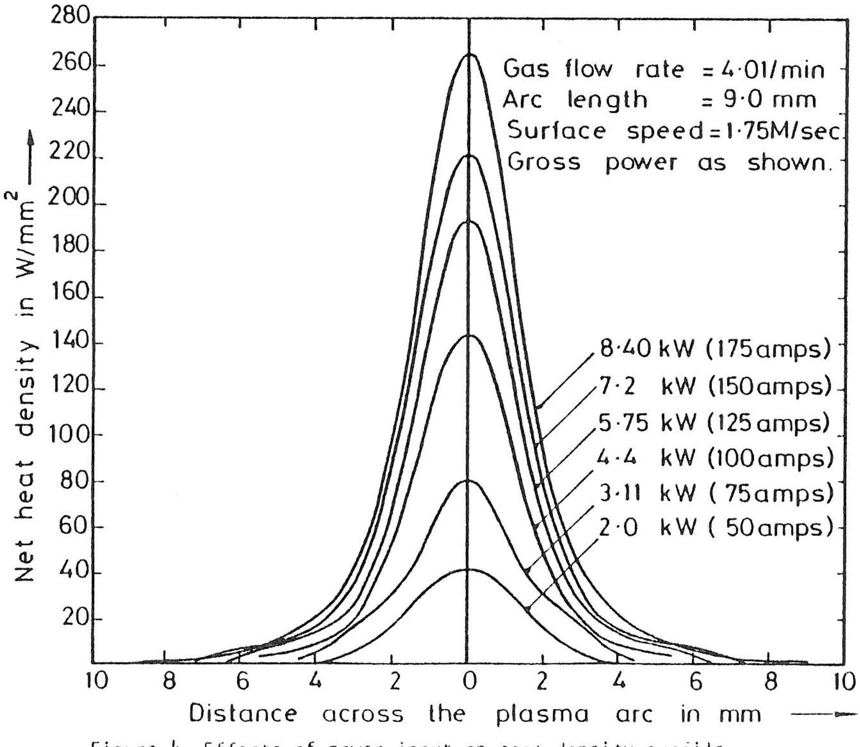

Figure 4 Effects of power input on heat density profile